EXPERIMENTAL INVESTIGATION OF THE FATIGUE BEHAVIOUR OF OFF-AXIS CFRP LAMINATES USING NON DESTRUCTIVE TECHNIQUES

Kalliopi-Artemi Kalteremidou[1], Sander Fonteyn[2,3], Delphine Carrella-Payan[4], Lincy Pyl[5] and Danny Van Hemelrijck[6]

[1] Department of Mechanics of Materials and Constructions, Vrije Universiteit Brussel (VUB), BE-1050 Brussels, Belgium, e-mail: Kalliopi-Artemi.Kalteremidou@vub.be, website: http://www.vub.ac.be/MEMC/
[2] Department of Mechanics of Materials and Constructions, Vrije Universiteit Brussel (VUB), BE-1050 Brussels, Belgium, e-mail: Sander.Fonteyn@vub.be, website: http://www.vub.ac.be/MEMC/
[3] SIM M3 Program, Technologiepark 935, B-9052 Zwijnaarde, Belgium, website: http://www.sim-flanders.be/research-program/m3
[4] Siemens Industry Software NV, Interleuvenlaan 68, B-3001 Leuven, Belgium, e-mail: delphine.carrella@siemens.com, website: http://www.siemens.com/plm/
[5] Department of Mechanics of Materials and Constructions, Vrije Universiteit Brussel (VUB), BE-1050 Brussels, Belgium, e-mail: Lincy.Pyl@vub.be, website: http://www.vub.ac.be/MEMC/
[6] Department of Mechanics of Materials and Constructions, Vrije Universiteit Brussel (VUB), BE-1050 Brussels, Belgium, e-mail: Danny.Van.Hemelrijck@vub.be, website: http://www.vub.ac.be/MEMC/

Keywords: Composite materials, Fatigue, Damage, Acoustic Emission, Digital Image Correlation

ABSTRACT

Composite materials are in practice subjected to fatigue loading, which most of the times happens to be multiaxial. This multiaxiality can for example appear in tubular specimens under combined tension/torsion loading or in cruciform specimens tested bi-axially. Due to the anisotropy that characterizes composite materials, multiaxial internal loads also occur even under simple uniaxial external loading. Therefore, it is preferable to use external uniaxial fatigue loading of flat coupons in order to study the local multiaxial fatigue behaviour of composites. In this study, Carbon Fibre Reinforced Epoxy (CFRE) flat specimens of two different lay-ups are tested under fatigue in different stress levels and R-ratios. 30º and 75º off-axis flat specimens are tested under uniaxial fatigue and the developed internal multiaxial loads are taken into account to investigate their influence on the fatigue behaviour of the material. Two different advanced monitoring methods, namely Digital Image Correlation (DIC) and Acoustic Emission (AE) are used during testing to clarify the damage processes.

1 INTRODUCTION

The use of composite materials is widely spread over the last decades. Their high mechanical and lightweight properties make them attractive for several applications, including automotive, aerospace and civil engineering. Many industrial fields make use of composite materials for highly stressed components, e.g. in bridges, wind turbine blades and automotive parts as they provide significant functional and economical benefits.

In general, composite components are subjected to multiaxial fatigue. In spite of its importance, the fatigue behaviour of composite materials under multiaxial stress state is difficult to be assessed and has not received much attention from the scientific community. Understanding the behaviour of composite materials under multiaxial dynamic loads is essential in order to design a high-performance material and create physically based models suitable to predict the fatigue life and damage [1-3].

Multiaxial loading can be applied in two ways: the first being the "external" multiaxiality, which is created by external loads in different directions while the second one is the "internal" multiaxiality,

which generates from the anisotropy of the composite material [4]. Normally, when it comes to study the fatigue behaviour of composite materials under multiaxial loads, it should not be necessary to distinguish between these two types of multiaxiality, as far as the local stresses in the material are the same. This is the reason why in order to study the fatigue of composite materials it is necessary to focus on local stresses, which means stresses in the material coordinates system, and not global or geometrical stresses [5]. The "external" multiaxiality can for example be applied by combined tension/torsion tests in cylindrical tubes or by bi-axial loading of cruciform specimens, whereas the "internal" multiaxiality is generated even in uniaxially loaded flat specimens [6-9]. As a first approach, flat specimens are preferably tested since the necessary equipment to perform uniaxial tests is much simpler and more easily available than the more complicated tools needed to perform tests on tubular or cruciform specimens.

Quaresimin et al. [10] suggested to use the bi-axiality ratios to describe the local multiaxial stress state acting on a lamina:

$$\lambda_1=\frac{\sigma_2}{\sigma_1},\ \lambda_2=\frac{\sigma_6}{\sigma_1},\ \ \lambda_{12}=\frac{\sigma_6}{\sigma_2} \tag{1}$$

where σ_1 and σ_2 are the longitudinal and transverse normal stress components and σ_6 is the in-plane shear stress in the material coordinates system. During their research they tested flat Glass Fibre Reinforced Polymer (GFRP) specimens under tension with a lay-up chosen so that the same λ_{12} is experienced as in tubes of different lay-up under external combined tension/torsion fatigue loading. They proved that the fatigue behaviour of the different geometries can be comparable as far as the local multiaxial stress state remains the same [10].

It has also been proven that the shear component appears to be detrimental for the fatigue behaviour of composite materials in terms of the fatigue life spent for the crack initiation, the crack propagation, the σ-N curves and the fracture surfaces [11]. For this reason special focus is given to λ_2 and λ_{12} bi-axiality ratios. Nevertheless, information is missing in the literature related to the fatigue damage behaviour of Carbon Fibre Reinforced Polymer (CFRP) material in terms of the local multiaxial stress states. Another challenging point in the case of CFRP material is that there is no transparency as in the case of the GFRP material so the evolution of the crack density cannot be easily used as a damage parameter without potentially usable instruments. Even if the stiffness degradation is a great damage indicator, the damage evolution of CFRP through the fatigue life is still not fully understood.

What one could also conclude based on a literature review is that the majority of the research on the multiaxial fatigue of composite materials concerns balanced and symmetric laminates [1], [4]. However, recent studies show that unbalanced laminates can make weight and cost benefits possible, thus it is of great importance to study the fatigue response of composite materials under multiaxial loading when it comes to the case of unbalanced laminates as well [12]. The unbalanced laminates consist of layers where the fibres are oriented in different directions but there is not always the negative counterpart $-\theta$ for every angle θ of the off-axis layers. Thus they are characterized by shear couplings, i.e. in-plane shear strains ε_{xy} that are developed even when simple normal stresses act on the laminate. In this case, the fibres' orientation influences a lot the mechanical performance of the laminates since different λ ratios are present in the local material coordinates system and also the tension-shear coupling of the off-axis laminates on the geometrical coordinates system has a significant impact on the fatigue behaviour of the material [13].

Taking all the above into consideration, this research deals with the uniaxial fatigue response of off-axis symmetric CFRP laminates consisting of layers with the same direction of the fibres in an angle θ with relation to the loading direction. As a first step of this research, two different angles are used for laminates with a $[\theta]_8$ lay-up, where θ is the angle that the fibres form with the loading direction. The different angle of the laminates induces different λ ratios during the uniaxial fatigue test and therefore the influence of the shear components σ_{12} on the fatigue behaviour can be analysed. Moreover, the different angle induces a different tension-shear coupling during testing. The aim of this research is to examine how the different multiaxial stress states and the tension-shear coupling influence the fatigue response of the CFRP material under different testing parameters by varying the stress levels and the R-ratios ($R=\sigma_{min}/\sigma_{max}$).

Apart from the examination of the mechanical response of the laminates under different fatigue testing parameters, Non Destructive Techniques (NDTs) are used to study the damage behaviour of the material [14]. NDTs are commonly applied to clarify the damage mechanisms in studies of composites. In the research presented here, the Digital Image Correlation (DIC) and Acoustic Emission (AE) technique are used to monitor the damage behaviour of the specimens. DIC is used to obtain the strain fields and AE to monitor the acoustic activity of the specimens during testing. The off-axis laminates are characterized by a sudden, brittle failure which doesn't allow us to study the macroscopic damage initiation and propagation by monitoring for example the crack density during testing. However, microscopic damage is being developed even from the beginning of the fatigue life. This microscopic damage evolves but is not able to directly cause the failure of the material. Only at the end of the fatigue life a crack resulting from the microscopic damage coalescences can propagate and result in the catastrophic failure of the material. Nevertheless, it is important to obtain an idea of the damage development in the laminates and correlate it with the lay-up of the laminate and the different testing parameters. The AE technique is able to "hear" the damage development of the laminates during testing [15]. AE can be used in two different ways. In the first way, the total acoustic activity during testing can be correlated with the testing parameters, i.e. the different stress levels and R-ratios, and the fatigue life. In the second way, the study of the features of the signals that are generated during the fatigue testing can be used in order to distinguish the different damage modes that appear during the fatigue test and examine how the different lay-up, the stress levels and the R-ratios induce different damage during testing [16], [17].

2 MATERIAL AND TESTING EQUIPMENT

2.1 Material

The material employed in the present study is composite laminates made of prepreg consisting of unidirectional (UD) carbon fibres and epoxy resin and manufactured by Mitsubishi Rayon Co., Ltd. The material is cured in compression moulding at a temperature of 140° C and a pressure of 8 MPa. Two different configurations of off-axis laminates with a lay-up $[\theta]_8$ are studied by using two different values of θ, namely 30° and 75°. The average thickness of the composite laminates for both angles is 1.83 mm. The cured ply elastic properties of the material are obtained by standard tests on $[0^o]_4$, $[90^o]_8$ and $[45^o/-45^o]_{2s}$ specimens of the material and are listed in Table 1.

Engineering constant	Unit	Value
$\sigma_{1,U}$	[MPa]	2272.43
$\sigma_{2,U}$	[MPa]	55.00
$\sigma_{6,U}$	[MPa]	52.27
E_1	[GPa]	125.83
E_2	[GPa]	9.40
G_{12}	[GPa]	4.06
ν_{12}	–	0.335
ν_{21}	–	0.029

Table 1**:** Elastic and strength properties of the composite material.

Off-axis test specimens were cut from 330 mm by 330 mm cured laminates. The shape and the dimensions of the specimens are based on the testing standard ASTM D3479 and they are shown in Figure 1. The total length of the specimens is l=250 mm, the gauge length l_g=150 mm, the width w=25 mm and the thickness t=1.83 mm. Rectangular-shaped tabs from thick paper were bonded on both ends of the specimens, which were sufficient to avoid stress concentrations in the tabbing area and to ensure a proper failure in the gauge length of the specimens.

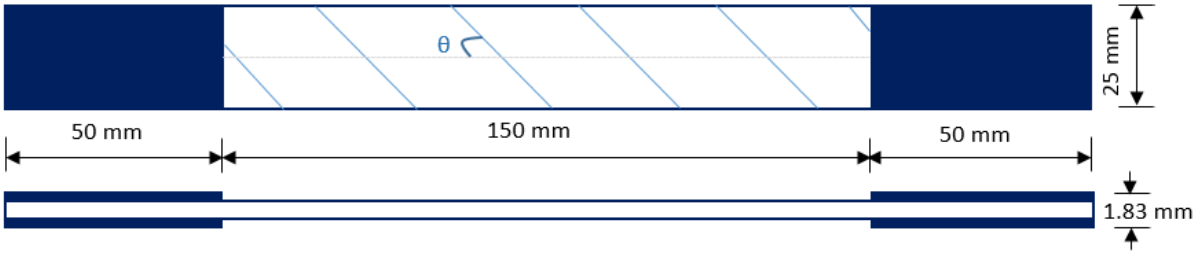

Figure 1: Specimen geometry.

As already mentioned, the aim of this research is to examine the influence of the λ ratios on the fatigue life and the damage response of the off-axis laminates. Especially the shear stress component has proven to be a dominant factor on the mechanical response of the composite laminates during fatigue. For this reason, special focus is given on the λ_{12} and λ_2 ratios. The bi-axiality ratios that are being developed in the off-axis layers are calculated using Classical Laminate Theory (CLT) and a numerical non-linear solver (Figure 2). More specifically, for the $[30^o]_8$ laminates, bi-axiality ratios of $|\lambda_{12}|=1.73$ and $|\lambda_2|=0.58$ are being generated in the off-axis layers, whereas for the $[75^o]_8$ laminates, bi-axiality ratios of $|\lambda_{12}|=0.27$ and $|\lambda_2|=3.73$ are being generated.

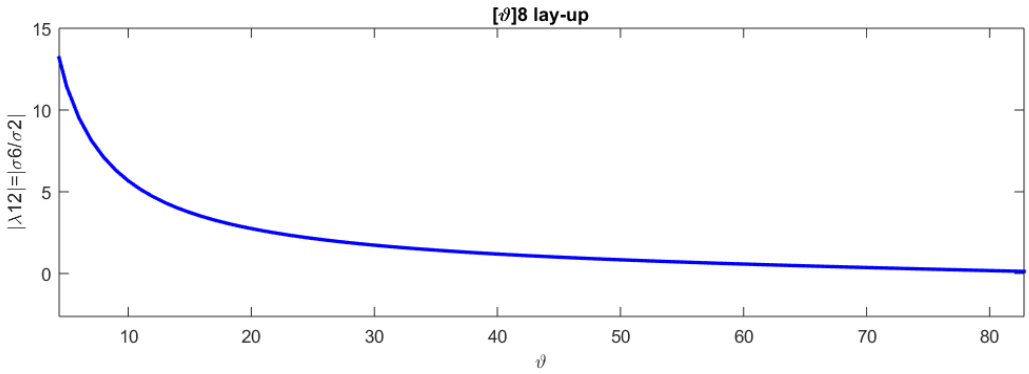

Figure 2: Variation of λ_{12} as a function of θ.

In both cases, the σ_1 component is in the same order of magnitude as the σ_2 and σ_6 components, which means it represents less than 4% of the ultimate strength of the laminates $\sigma_{1,u}$ supporting the conclusion that the behaviour is matrix dominated, mainly affected by the transverse and the shear stresses. The last point is important because it is more convenient as a first approach to uncouple the results from the contribution of the fibres on the mechanical behaviour and only study how the transverse and shear stresses, which are dominant, influence the fatigue response.

What one should also take into consideration in the case of $[\theta]_n$ off-axis laminates is the tension-shear coupling, which means that in-plane shear strains ε_{xy} are developed even under uniaxial tensile forces N_x. In the case of the $[30^o]_8$ laminates the A_{xy} term of the extensional stiffness matrix A from the constitutive equation, representing the relation of the normal forces with the in-plane shear strains, is equal to A_{xy}=69.07 GPa*mm, while for the $[75^o]_8$ the same term is A_{xy}=4.17 GPa*mm. Therefore it is of high importance to see how this difference of 94% in the tension-shear coupling influences the fatigue behaviour of the laminates.

The objective is to correlate the multiaxial λ ratios on the material coordinates system and the magnitude of the tension-shear coupling on the geometrical coordinates system with the fatigue behaviour of the off-axis laminates. After this step, UD lay-ups with different values for the angle θ can be tested and finally the full characterization of off-axis laminates under fatigue loads and under different testing parameters can be achieved.

2.2 Testing equipment

In order to characterize the fatigue behaviour of the off-axis laminates, static tests were initially performed before the fatigue tests with a 1 mm/min displacement rate and with three repetitions for each lay-up. All the tests were performed using a servo-hydraulic test machine with mechanical grips and a load cell of 10 kN capacity for static tests and 5 kN capacity for fatigue tests. Cyclic loads were applied under load control with a frequency of 3 Hz. The cycles were sinusoidal and two different R-ratios ($R=\sigma_{min}/\sigma_{max}$), namely 0.1 and 0.5 were applied. Three different percentages of the ultimate strength of the off-axis laminates, 70%, 80% and 90%, were used as the maximum stress level σ_{max} for the fatigue tests. The two different R-ratios and the three stress levels lead to six different categories of fatigue tests for each lay-up and at least three specimens were tested for each category, which results in a total amount of 36 tests under different fatigue parameters. The "run-out" for the fatigue tests was set to 10^6 cycles.

The strains during testing were measured using a 50 mm extensometer. At the same time, a Digital Image Correlation system VIC-3D by Correlated Solutions with two camera lenses was used in order to obtain the full-field strain maps during testing through triangulation of the two cameras. A random black-white speckle pattern was applied on the specimens using aerosol paint and by capturing regular images of the surface of the specimens, the in-plane strains of the specimens were calculated. For the static tests, images were captured every 1 second during testing and for the fatigue tests the Fulcrum add-on was used. In this way, images were captured at the peaks of a cycle, i.e. at the maximum and the minimum stress of a cycle. For the "short" tests where the fatigue life was less than 5000 cycles, images were captured every 10 cycles during the fatigue life, while for the longer tests images were captured every 10 cycles in the beginning of the fatigue life and progressively every 100 and every 1000 cycles until the end of the test.

In order to monitor the acoustic activity during the tests, an eight-channel DiSP system by Physical Acoustics was used. Two piezoelectric transducers (Pico) with a broadband response and maximum sensitivity at 450 kHz were mounted on the specimen using Vaseline grease. The received signals were amplified using preamplifiers with a uniform gain of 40 dB and a 35 dB threshold was applied in order to filter out the noise of the mechanical system. Before testing, lead break tests were carried out in order to check the sensibility of the transducers and to calculate the surface wave speed, which is 4000 m/sec for the $[30^o]_8$ laminates and 2500 m/sec for the $[75^o]_8$ laminates.

The set-up of the mechanical system and the equipment for the NDTs is shown in Figures 3 and 4. In Figure 4 the transducers, the extensometer and the speckle pattern that was painted on the specimens for the DIC technique are shown.

Figure 3: Test set-up.

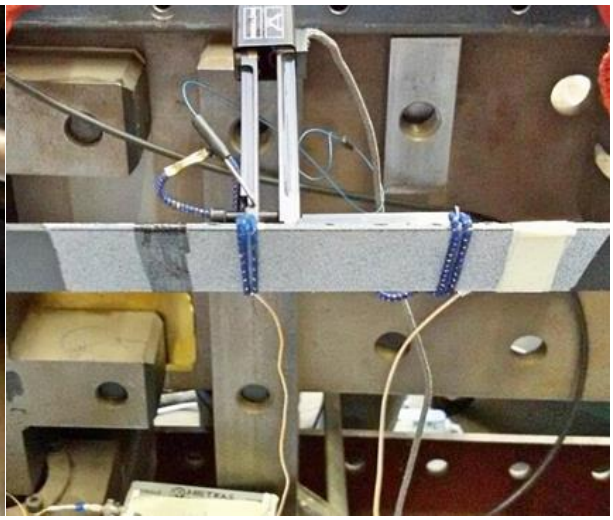

Figure 4: Sensors, extensometer and speckle pattern attached on the specimen.

3 RESULTS AND DISCUSSION

3.1 Static tests

Before the analysis of the fatigue tests, the interpretation of the static tests for the two off-axis $[30^o]_8$ and $[75^o]_8$ UD lay-ups is important. Since the maximum load during the fatigue cycles is a specific percentage of the ultimate static strength averaged value, it is necessary to obtain the stress-strain graphs for the laminates in order to examine how the material behaves during the static loading and to calibrate the AE system. In Figure 5, the stress-strain graphs for the two different laminates are presented. Of course, as expected from mechanics of composites, the $[30^o]_8$ laminates result in higher ultimate strength and higher strain to failure in comparison with the $[75^o]_8$ laminates. In Table 2 the average mechanical properties of the laminates are presented. For the calculation of the E-modulus E_x, the part of the curves that corresponds to strains from 0.1% to 0.3% was used based on the testing standard ASTM D3039.

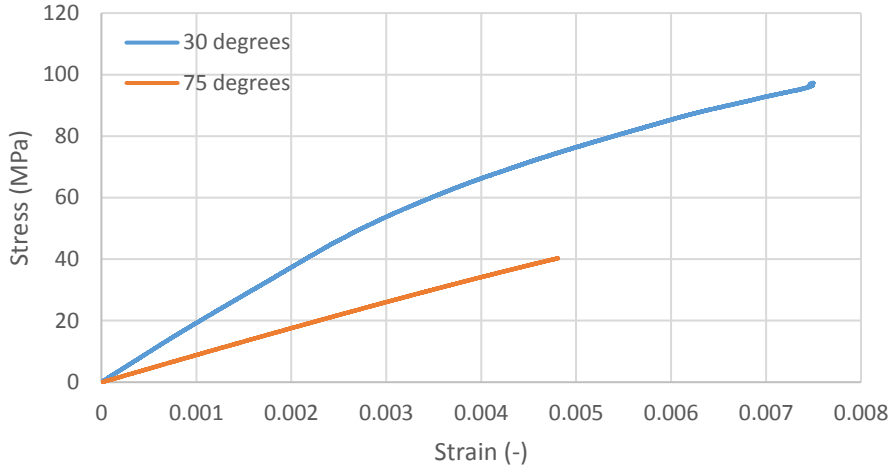

Figure 5: Stress-Strain curves of the off-axis laminates.

Engineering constant	Unit	$[30^o]_8$	$[75^o]_8$
$\sigma_{x,u}$	[MPa]	104.47	40.52
E_x	[GPa]	16.65	8.56
$\varepsilon_{x,u}$	[%]	0.78	0.44

Table 2: Mechanical properties of the off-axis laminates.

Both lay-ups are characterized by a brittle behaviour, however the stress-strain curve of the $[75^o]_8$ laminates is totally linear, while the $[30^o]_8$ laminates show a small non-linearity during the static loading, which starts at a stress value around 62% of the ultimate strength. This is resembled also in the total acoustic activity during the static test recorded by the AE software. In Figures 6 and 7 the acoustic activity in relation with the stress for the $[30^o]_8$ and $[75^o]_8$ lay-ups respectively is presented. While for the $[75^o]_8$ lay-up the acoustic activity increases progressively with a big increase near the end of the test, the $[30^o]_8$ laminates show a different behaviour where the acoustic activity slowly increases during the linear part of the stress-strain curve and a big increase is appearing exactly at 62% of the ultimate strength, where the non-linearity appears. This behaviour is appearing for each one of the three repetitions of the static tests performed.

For both lay-ups, two different kinds of signals are obtained by the AE software. One part of the acoustic signals can be attributed to small matrix cracks occurring during testing. However, the energy appearing is not sufficient in order for the cracks to propagate and to provoke the total failure of the specimen. The other part of the signals is related to the fibre/matrix decohesions that are mostly caused by the shear strains that increase during the static test. In the case of the $[75^o]_8$, mostly the first type of acoustic hits is present during testing and only a small number of hits is recorded for a very big part of

the test. Close to the failure of the material, the acoustic activity increases with mostly small matrix cracks and a few decohesions occurring until the final failure of the specimen. For the $[30^o]_8$ laminates, mostly the first type of signals related to matrix cracks is appearing with a low rate until the stress reaches a stress equal to 62% of the ultimate strength and the non-linear behaviour starts. At that point, the rate increases suddenly and apart from the first type of hits, a lot of signals related with the second damage mode of decohesions appear until the failure of the material. As the shear strains increase, more and more shear decohesions occur resulting in the increase of the total acoustic activity and the appearance of the second type of hits.

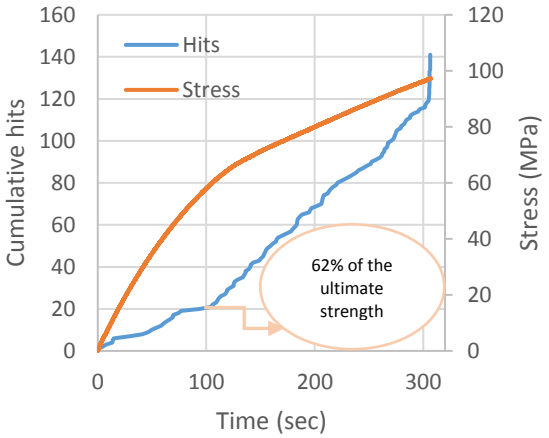

Figure 6: Acoustic activity for $[30^o]_8$ laminates.

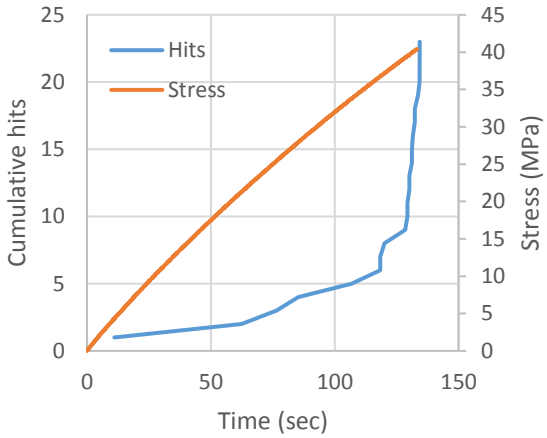

Figure 7: Acoustic activity for $[75^o]_8$ laminates.

3.2 Fatigue tests

The mechanical response and the acoustic activity during the fatigue tests of the different laminates strongly depends on the maximum stress and R-ratio applied and on the angle of the fibres since different stresses and thus damage modes are developed for the different lay-ups. Regarding the fatigue response of the laminates, Figures 8 and 9 show the σ-N curves of the two laminates for the two different R-ratios that were used, namely 0.1 and 0.5, obtained by logarithmic fitting. For the $[30^o]_8$ laminates, there is no overlap between the two curves corresponding to the different R-ratios. One can notice that the fatigue life is longer for R=0.5 for all stress levels with even a "run-out" when the maximum applied stress is 70% of the ultimate strength. For R=0.1 the fatigue life is shorter and especially for 70% of the ultimate strength the fatigue life is 99% shorter in comparison with R=0.5, with the fatigue life being in a magnitude of 10000 cycles for R=0.1.

A different behaviour is noticed for the $[75^o]_8$ laminates. In this case, the influence of the R-ratio on the fatigue life depends on the maximum stress applied during the test. For 70% of the ultimate strength, the response is the same with the $[30^o]_8$ laminates with the R-ratio of 0.5 resulting again in "run-out" and the ratio of 0.1 leading to a 90% shorter fatigue life. However, this time the difference between the two ratios is smaller than in the $[30^o]_8$ laminates, since for R=0.1 the fatigue life reaches about 100000 cycles. For σ_{max} equal to 80%, the smaller R-ratio results in a 85% shorter fatigue life than the higher R-ratio, but also in this case the difference is smaller than in the case of the $[30^o]_8$ laminates. The difference between the two lay-ups is even more obvious in the higher maximum applied stress of 90%, where a ratio of 0.5 leads to a 93% shorter fatigue life than a ratio of 0.1.

It is obvious that the laminates exhibit a different fatigue behaviour, which should be attributed to the orientation of the fibres and the different stress states that are developed and that lead to different damage modes. Considering the fatigue life of the material for the two lay-ups, we can see that in any combination of stress level and R-ratio, the $[75^o]_8$ laminate always exhibits longer fatigue life than the $[30^o]_8$. During loading, the $[75^o]_8$ laminate has a λ_{12} ratio equal to 0.27, while the $[30^o]_8$ one has a value of 1.73. This means that the bigger shear stresses that are present in the second laminate influence a lot the fatigue response and reduce the fatigue life of the material. The $[75^o]_8$ exhibits a better fatigue response even if the ultimate static strength is lower than the $[30^o]_8$, since the failure is dominated by

the transverse stresses. In the $[30^o]_8$ laminates the failure is dominated by the shear stresses and we can conclude that the shear stresses are indeed a detrimental factor in the fatigue behaviour of the composite material.

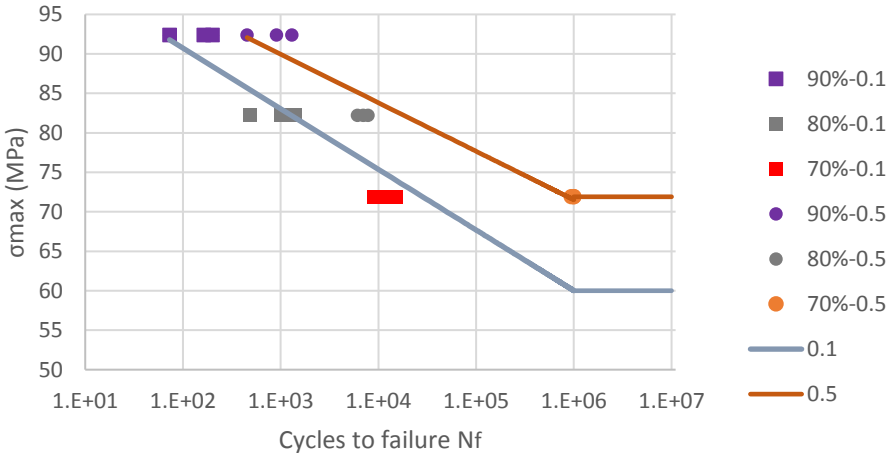

Figure 8: σ-N curves for $[30^o]_8$ laminates.

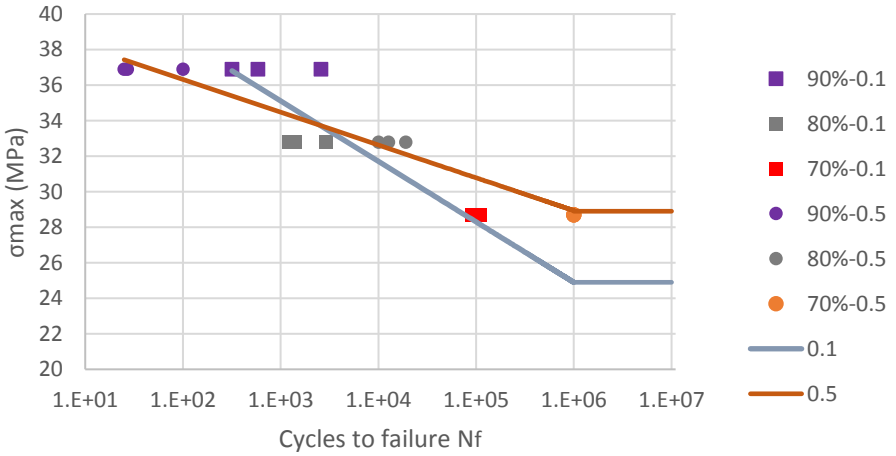

Figure 9: σ-N curves for $[75^o]_8$ laminates.

Examining now how the testing parameters influence the fatigue life, it can be noted that the $[75^o]_8$ laminates seem to be more sensitive to the combination of the applied maximum stress and the R-ratio, while the $[30^o]_8$ laminates are more sensitive on the value of the R-ratio when a specific stress level is considered, since the difference in the fatigue life between the two different values of the R-ratio is higher. The sensitivity of the latter lay-up on the influence of the R-ratio on the fatigue life can also be related to the λ ratios developed in the laminate.

The smaller R-ratio means that fatigue cycles with a higher amplitude are applied on the material. In the case of the angle of 30°, this results in the fact that during fatigue the stresses are continuously varying in a big range moving from the linear part of the stress-strain curve to the non-linear one. In the transition between these parts, the changes in the shear stresses σ_6 and in the ε_{xy} strains occurring from the extension-shear coupling of the laminates are big. This can be seen in Figures 10 and 11 where the shear strains that occur between two consecutive cycles for a 90%-0.1 fatigue test obtained from the DIC software are shown. The big difference in the shear strains shows that apart from the development of micro-cracks in the matrix, big shear decohesions between the fibres and the matrix appear because the material is getting more "exhausted" from the big variations in the shear strains. In the high R-ratio case, the amplitude is lower and thus the shear stresses and strains that are developed from the minimum to the maximum applied stress are similar and this results in longer fatigue lives.

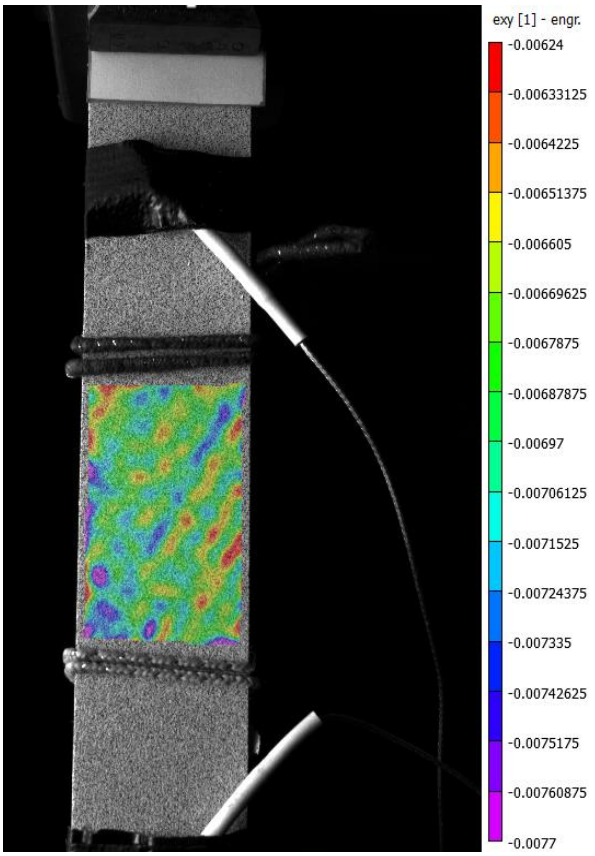

Figure 10: Shear strains at the maximum peak of a cycle for a 90%-0.1 test of a $[30^o]_8$ laminate.

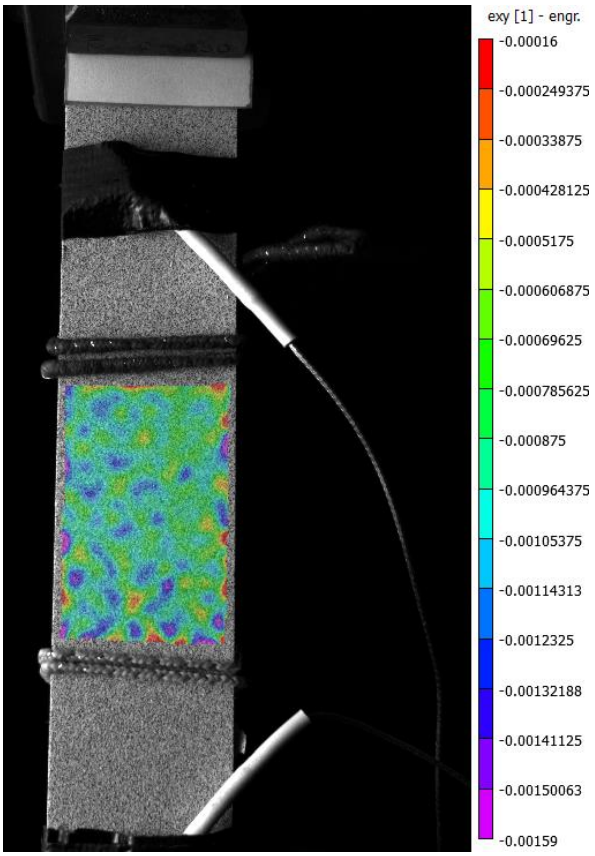

Figure 11: Shear strains at the minimum peak of a cycle for a 90%-0.1 test of a $[30^o]_8$ laminate.

For the case of the $[75^o]_8$ laminates we notice in Figure 9 that the combination of the maximum applied stress with the R-ratio is the biggest factor that influences the fatigue life. For a specific stress level, the two R-ratios lead to a smaller difference in the fatigue life than in the case of $[30^o]_8$ laminates, with the fatigue life being 10 times shorter for R=0.1 compared to R=0.5 for 70% of the ultimate strength, but being around 13 times shorter for R=0.5 compared to R=0.1 for a maximum applied stress equal to 90% of the ultimate strength. The reason behind this can be the fact that the behaviour of the $[75^o]_8$ laminates is linear and driven by the transverse stresses and thus the main damage mode is matrix micro-cracks. In a maximum stress level equal to 70% of the ultimate strength, the matrix cracks occurring in the beginning of the fatigue life are not able to propagate and to cause the catastrophic failure of the material. In this case, a higher R-ratio with a smaller amplitude during loading leads to long fatigue life since the stress range is small and the opening and closure of the present matrix cracks is not so quick as in the case of the smaller stress ratio. We notice that this tendency is reduced as the maximum stress increases. For a stress equal to 80% of the ultimate strength, the difference in the fatigue life between the two R-ratios is reduced and for 90% the tendency is even inversed, with a higher fatigue life for R=0.1.

In order to better understand and explain the fatigue response of the off-axis laminates in correlation with the testing parameters, in Figures 12 and 13 the total acoustic activity during testing for the $[30^o]_8$ laminates and the $[75^o]_8$ laminates respectively is plotted versus the percentage of the fatigue life. Due to space limitations, only the results for R=0.1 are shown since for this stress ratio smaller fatigue lives are achieved and thus bigger damage during the fatigue test appears. From a first view we can see that the $[30^o]_8$ laminates show a much higher acoustic activity during the fatigue test in comparison with the $[75^o]_8$ laminates for the three different maximum stress levels. This means that the influence of the shear strains and the λ ratios on the fatigue response is resembled also on the difference in the acoustic activity during the test apart from the σ-N curves.

The higher acoustic activity for the $[30^o]_8$ laminates during the test can be attributed to the two different damage modes that appear during the test. While in the $[75^o]_8$ laminates the main damage mode is matrix micro-cracks that are not able to cause the total failure of the specimen, in the $[30^o]_8$ laminates shear decohesions are the dominant damage mode creating a lot of acoustic activity during the test. This is also obvious when we compare the total cumulative hits for the different maximum stress levels for the $[30^o]_8$ laminates. Starting from a maximum applied stress equal to 70% of the ultimate strength and reaching a value of 90%, it is obvious that the acoustic response increases rapidly. The difference in the cumulative hits between the 3 stress levels is high and especially the difference between the 80% and the 90% maximum applied stress shows how a small increase in the applied load and in the developed shear stresses and strains results in a big activation of the damage mode of shear decohesions. For the case of the $[75^o]_8$ laminates, an increase in the acoustic activity is also obvious when the maximum applied stress increases but the difference is not so high as in the first lay-up. The increase in the cumulative hits can be attributed to the increase of matrix cracks occurring during loading.

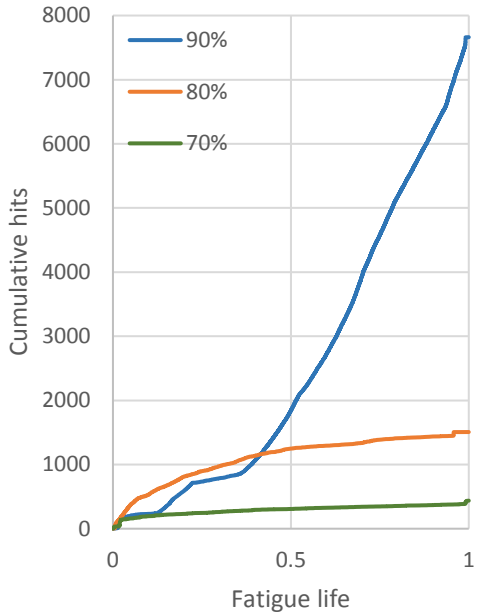

Figure 12: Acoustic activity of $[30^o]_8$ laminates for R=0.1 and 3 different maximum stresses.

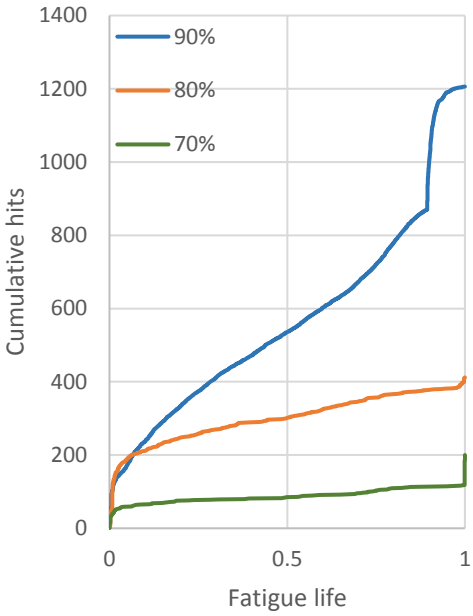

Figure 13: Acoustic activity of $[75^o]_8$ laminates for R=0.1 and 3 different maximum stresses.

In order to correlate the acoustic activity during the fatigue tests with the mechanical response of the material, the stiffness degradation of the specimens for the three maximum applied stresses and for R=0.1 is plotted in Figure 14 for the $[30^o]_8$ laminates and in Figure 15 for the $[75^o]_8$ laminates. We can notice that generally the stiffness degradation is very small for all the cases as is expected for brittle materials. However, it is obvious the difference in the stiffness degradation for the different maximum applied stresses. For both lay-ups, higher maximum stress results in bigger stiffness degradation. A maximum applied stress of 90% of the ultimate static strength leads to a drop of around 9% for the $[30^o]_8$ laminates while it results in a less than 4% stiffness degradation for the $[75^o]_8$ laminates. This is in relation with the high acoustic activity that is developed for the higher stresses, since the higher applied loads lead to more damage in a shorter period. Especially for the $[30^o]_8$ laminates, where two different damage modes are present, the difference in the stiffness degradation is even bigger with a difference of around 7% between the 70% and the 90% maximum applied stress since a small increase in the magnitude of the shear strains leads to big differences in the acoustic activity and the stiffness degradation.

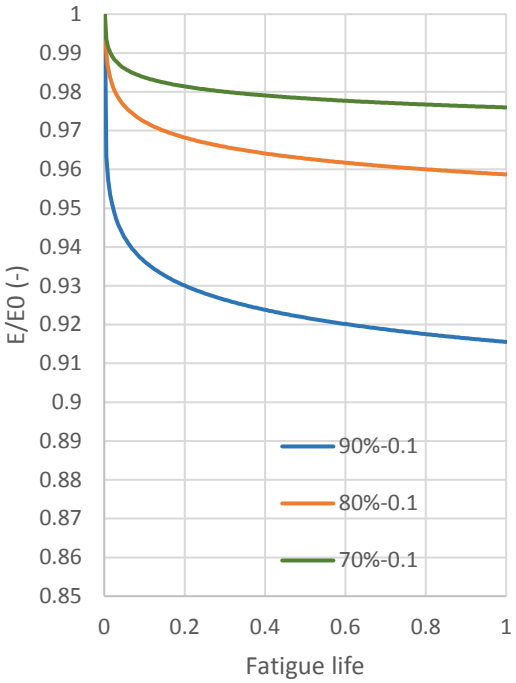

Figure 14: Stiffness degradation of $[30^o]_8$ laminates for R=0.1 and 3 different maximum stresses.

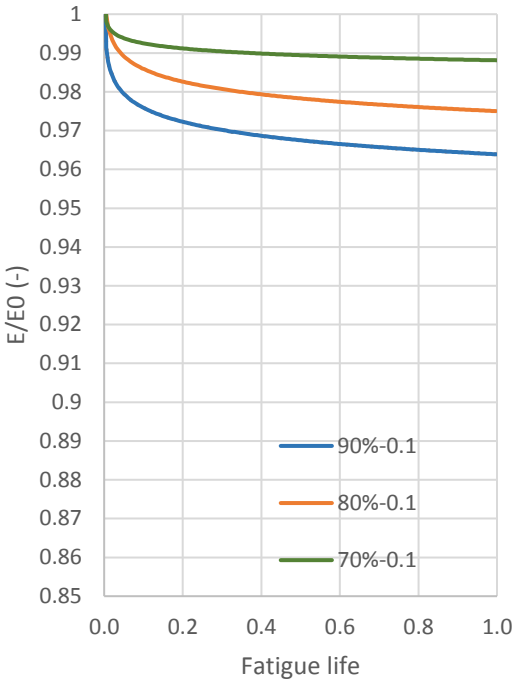

Figure 15: Stiffness degradation of $[75^o]_8$ laminates for R=0.1 and 3 different maximum stresses.

4 CONCLUSIONS

During the first step of this research, off-axis CFRP laminates with a lay-up $[\theta]_8$ for two different values of θ were tested under fatigue under different stress levels and stress ratios. It is proven that the different stresses and strains occurring for the different laminates and represented by the bi-axiality λ ratios lead to different damage modes which influence in a different way the fatigue response of the material. An increase in the λ_{12} ratio from 0.27 for the $[75^o]_8$ laminates to 1.73 for the $[30^o]_8$ laminates results in shorter fatigue life, higher acoustic activity and bigger stiffness degradation during fatigue. In the case where the transverse stresses are dominant as in the case of the $[75^o]_8$ laminates and thus the matrix micro-cracks is the main damage mode, the fatigue behaviour is better in terms of the length of the fatigue life and the stiffness degradation and the acoustic activity is limited during the test, with a maximum loss of less than 4% of the stiffness during the fatigue. The combination of the R-ratio and the maximum stress seems to influence the fatigue life of the $[75^o]_8$ laminates. When the λ_{12} ratio and the tension-shear coupling increase as in the case of the $[30^o]_8$ laminates, the shear stresses and strains prove to be detrimental for the fatigue response. In this case, apart from the matrix cracks, shear develops in the interface of the matrix with the fibres. Even a small increase in the maximum applied stress and thus in the shear strains results in a decrease in the fatigue life and in higher stiffness degradation. This is also resembled in the acoustic activity during the test, where a lot of acoustic hits are recorded attributed to the matrix cracks but mostly to the shear decohesions.

ACKNOWLEDGEMENTS

The work leading to this publication has been funded by the SBO project "M3Strength", which fits in the MacroModelMat (M3) research program funded by SIM (Strategic Initiative Materials in Flanders) and VLAIO (Flanders Innovation & Entrepreneurship Agency). The authors gratefully acknowledge the material suppliers Mitsubishi Rayon Co., Ltd and Honda R&D Co., Ltd. The authors would also like to thank the financial support of the Fonds Wetenschappelijk Onderzoek (FWO) research funding program "Multi-scale modelling and characterisation of fatigue damage in unidirectionally reinforced polymer composites under multiaxial and variable-amplitude loading".

REFERENCES

[1] A.S. Chen and F.L. Matthews, A review of multiaxial/biaxial loading tests for composite materials, *Composites*, **24**, 1993, pp. 395–406.

[2] A. Carpinteri, M. De Freitas and A. Spagnoli, *Biaxial/Multiaxial fatigue and fracture*, Vol. 31, 2001.

[3] M. Quaresimin and L. Susmel, Multiaxial Fatigue Behaviour of Composite Laminates, *Key Engineering Materials*, **221–222**, 2002, pp. 71–80.

[4] M. Quaresimin, 50th anniversary article: Multiaxial fatigue testing of composites: From the pioneers to future directions, *Strain*, **51**, 2015, pp. 16–29.

[5] M. Quaresimin and P.A. Carraro, Damage initiation and evolution in glass/epoxy tubes subjected to combined tension-torsion fatigue loading, *International Journal of Fatigue*, **63**, 2014, pp. 25–35.

[6] C.S. Lee, W. Hwang, H.C. Park and K.S. Han, Failure of carbon/epoxy composite tubes under combined axial and torsional loading 2. Fracture morphology and failure mechanism, *Composites Science and Technology*, **59**, 1999, pp. 1789–1804.

[7] S.R. Swanson, A.P. Christoforou and G.E. Colvin, Biaxial testing of fiber composites using tubular specimens, *Experimental Mechanics*, **28**, 1988, pp. 238–243.

[8] A. Smits, D. Van Hemelrijck, T.P. Philippidis and A. Cardon, Design of a cruciform specimen for biaxial testing of fibre reinforced composite laminates, *Composites Science and Technology*, **66**, 2006, pp. 964–975.

[9] A.E. Antoniou, D. Van Hemelrijck and T.P. Philippidis, Failure prediction for a glass/epoxy cruciform specimen under static biaxial loading, *Composites Science and Technology*, **70**, 2010, pp. 1232–1241.

[10] M. Quaresimin, P.A. Carraro, L.P. Mikkelsen, N. Lucato, L. Vivian, P. Brondsted, B.F. Sorensen, J. Varna and R. Talreja, Damage evolution under cyclic multiaxial stress state: A comparative analysis between glass/epoxy laminates and tubes, *Composites Part B: Engineering*, **65**, 2014, pp. 2–10.

[11] V.G. Perevozchikov, V.A. Limonov, V.D. Protasov and V.P. Tamuzh, Static and fatigue strength of unidirectional composites under the combined effect of shear stress and transverse tension-compression stresses, *Mechanics of Composite Materials*, **24**, 1989, pp. 638-644.

[12] S.W. Tsai, Weight and cost reduction by using off-axis and unsymmetric laminates, *Proceedings of the 18th International Conference on Composite Materials ICCM18, Jeju, Korea, August 21-26, 2011*.

[13] M. Kawai, S. Yajima, A. Hachinohe and Y. Takano, Off-axis fatigue behavior of unidirectional carbon fiber-reinforced composites at room and high temperatures, *Journal of Composite Materials*, **35**, 2001, pp. 545-576.

[14] J. Cuadra, P.A. Vanniamparambil, K. Hazeli, I. Bartoli and A. Kontsos, Damage quantification in polymer composites using a hybrid NDT approach, *Composites Science and Technology*, **83**, 2013, pp. 11–21.

[15] D.G. Aggelis, N.M. Barkoula, T.E. Matikas and A.S. Paipetis, Acoustic emission monitoring of degradation of cross ply laminates, *Journal of the Acoustical Society of America*, **127**, 2010, pp. 246-251.

[16] N. Godin, S. Huguet, R. Gaertner and L. Salmon, Clustering of acoustic emission signals collected during tensile tests on unidirectional glass/polyester composite using supervised and unsupervised classifiers, *NDT & E International Journal*, **37**, 2004, pp. 253–264.

[17] P. Nimdum and J. Renard, Use of acoustic emission to discriminate damage modes in carbon fibre reinforced epoxy laminate during tensile and buckling loading, *Proceedings of the 15th European Conference on Composite Materials ECCM15, Venice, Italy, June 24-28, 2012.*